

## Beam Performance and Upgrades of the Storage Ring

### Orbit Stability

In 2002, it was accomplished the suppressing of chamber vibration in quadrupole magnets reducing drastically the fast variation of the beam orbit in the storage ring [1]. However, the slow drift of orbit is still large. The beam orbit moves slowly within  $\pm 10 \mu\text{m}$ , which generates about  $1.5 \mu\text{rad}$  in angle of the photon beam axis at the worst case. From the observation of the orbit drift, we found that the shortage of degrees of freedom in the steering phase causes this drift. After many orbit correction steps, the higher order distortion of the orbit is created. The periodic correction was carried out using the twenty-four air-core-type steering magnets with high resolution and low hysteresis. We therefore investigated the possibility of using normal horizontal and vertical steering magnets (six horizontal and vertical steering magnets are usually installed in each Chasman-Green cell) to increase the available number of steering in the correction. The problem is the poor resolution of field setting, which is two orders worse than that of the air-core-type steering magnets. To reduce the field setting errors while using the normal steering magnets, we investigated the magnets' hysteresis. Results show that the hysteresis is not so large and the resolution of the field setting can be drastically improved by increasing the resolution of the current setting in the power-supplies.

On the other hand, when many steering magnets are used in the correction, the photon beam axis of each beamline is necessary for keeping all the axes constant. To this end, to ensure the absolute transverse positions of the attached BPMs which are installed upstream and downstream of insertion devices (IDs), we have designed a set of new chambers equipped with BPM. The readouts from BPMs define the corresponding photon axis. Three sets of new

BPM chambers have been installed in three ID straight sections and their performances is being investigated. The GUI program for the periodic orbit correction has also been modified to consider all photon axes of ID beamlines. The new algorithm will be in service in May 2004.

### Top-up Operation

The top-up operation maximizes research activities in a synchrotron radiation (SR) facility by an effectively infinite beam lifetime and high photon beam stability. We have been improving the SPring-8 accelerators to achieve the ideal top-up operation. Since autumn 2003, we have been injecting the beams keeping the photon beam shutters opened and ID gaps closed. We are developing a bunch-by-bunch feedback system to reduce further the beam loss with all the ID gaps fully closed by lowering the operating chromaticity. The top-up operation with constant stored current is scheduled in May 2004. This operation requires two key conditions. One is a perturbation-free injection, which never perturbs users' experiments by exciting the oscillation of stored beams. Figure 1 shows effective beam size variations due to the beam injection before improvements, which are measured at a beam diagnosis beamline by the X-ray beam profile monitor. The betatron

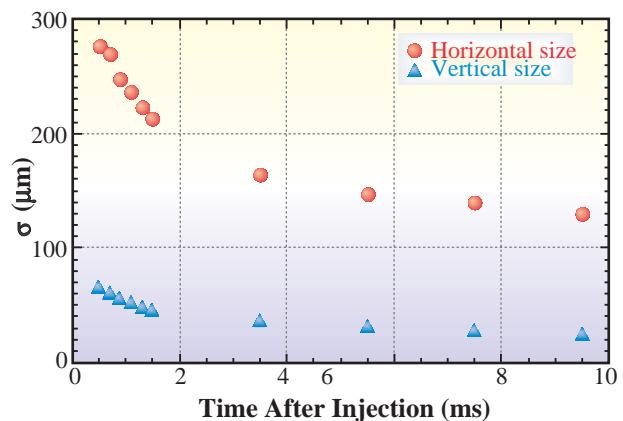


Fig. 1. Horizontal and vertical beam size variations due to the beam injection before improvements.

functions are 2.1 m and 27.8 m in horizontal and vertical directions, respectively. The other is a loss-free injection, which prevents demagnetization of permanent magnets comprising of IDs through the lost electron bombardment.

In order to reduce the amplitude of the horizontal oscillation, we have adjusted the magnetic field shape of four injection bump magnets to close the bump orbit. Since the eddy current at the end plates of magnets mainly causes the similarity break of the field shape, the four bump magnets were replaced by the new ones having the nonmetal end plates to reduce the effect of the eddy current [2]. We also developed a scheme for suppressing the horizontal oscillation induced by the nonlinearity of sextupole magnets. This scheme can make the oscillation amplitude negligibly smaller than the horizontal beam size, down to a few tens microns by a simple optimization of sextupole strengths in the injection bump [3]. These reduced the horizontal oscillation down to one-third of the stored beam size. Figure 2 shows the time variation of the horizontal oscillation amplitude of the stored beam.

The vertical oscillation of the stored beam is excited depending on the amplitude of the injection bump, which reveals that the tilt of the bump magnets causes the vertical oscillation.

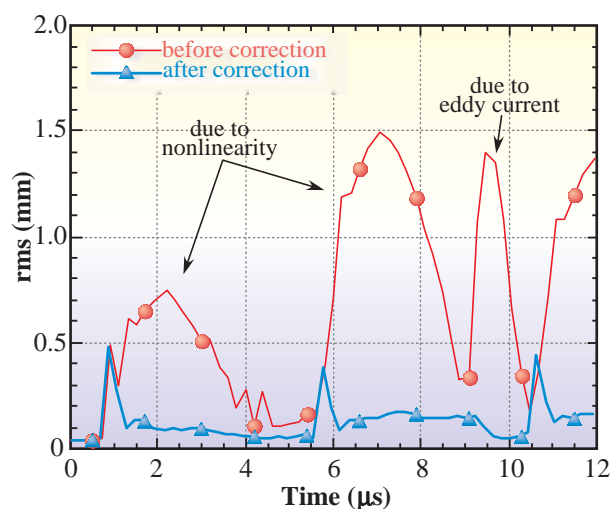


Fig. 2. Horizontal oscillation amplitude of stored beam measured using turn-by-turn monitor.

By adjusting the tilt angle of bump magnets properly, the vertical oscillation was reduced by one-third. For the remaining vertical oscillation, the feedforward correction was applied with a single pulse corrector. These two countermeasures reduced the vertical oscillation down to two-thirds of the stored beam size. As a result of the above suppression treatments, the variation of monochromatized beam intensity has become less than 10% at the experimental station during the beam injection.

For the loss-free injection, beam collimators were installed upstream of the beam transport line from the booster synchrotron. The horizontal tail of the injection beam is usually cut at  $\pm 1\sigma$  and the core part of the beam is only injected to the storage ring. This realized the injection efficiency of nearly 100% under the restricted gap condition of in-vacuum IDs [4].

### Bunch-by-bunch feedback

Transverse beam instabilities are one during the most serious problems during the operation of the SPRING-8 storage ring, and to suppress them, a large chromaticity was introduced to the ring optics. However, this large chromaticity imposes a serious restriction on the ring operation and it is difficult to optimize ring parameters for recently requested advanced operation modes, such as top-up, high-current and low-energy modes. To dissolve this large chromaticity, a bunch-by-bunch feedback system (BBF) is developed and its introduction to user operation is scheduled at the start of 2004. The BBF is another method for curing instabilities and this measures the positions of bunches and kicks them back bunch-by-bunch, turn-by-turn. A block diagram of the BBF system is shown in Fig. 3.

Compared with similar systems in other facilities, our BBF system has several advantages: low-noise high-resolution position detection and digitization, and nearly one-order-lower cost by using of FPGAs instead of DSPs for digital signal processing. To reduce the noise of the system, a fast and high-resolution strip-line monitor was developed and slow but high-

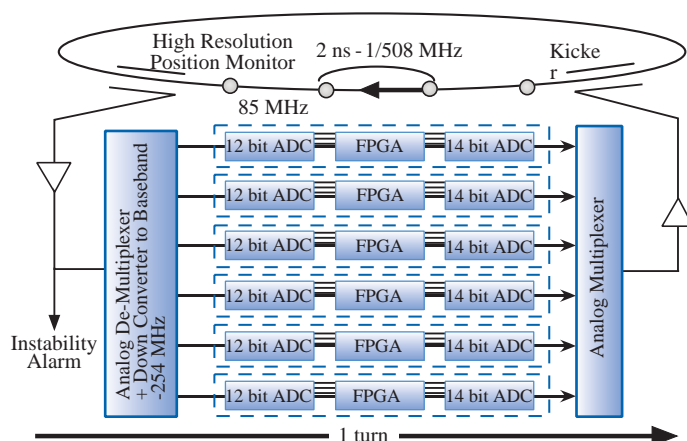


Fig. 3. Schematic block diagram of the bunch-by-bunch feedback system.

resolution ADCs were employed with the help of a newly invented analog de-multiplexer. The diagnosis system of the BBF and the instability detection and alarm system were also developed.

### Accelerator Diagnosis Beamlines

X-ray imaging observation of the electron beam using a zone plate X-ray beam profile monitor [5] is in progress at the accelerator diagnosis beamline #1 (BL38B2). The focused image of the electron beam was successfully obtained. Figure 4 shows an example of images of the electron beam of the SPring-8 storage ring observed using this monitor. The operation conditions of the ring are as follow: low-emittance optics, multi-bunch filling, beam current of 100 mA, and all ID gaps fully open. On the basis of preliminary calibrations of the X-ray zooming tube, the horizontal and vertical beam sizes ( $1\sigma$ ) were roughly  $120\ \mu\text{m}$  and  $15\ \mu\text{m}$ , respectively. Equipments for use in SR experiments on accelerator components were installed in the optics hutch of BL38B2. The installed equipments are a vacuum chamber for irradiation experiments of photon absorbers, metal filters for controlling irradiating SR intensity, and Be windows through which white X-ray radiation exits into the atmosphere. For example, radiation damage of insulators of quadrupole

magnets was studied using white radiation in the atmosphere.

Construction of the accelerator diagnosis beamline #2 (BL05SS) is in progress. In 2003, the UHV components of the front end were installed in the accelerator tunnel. The radiation shielding hutches were built on the experimental hall. BL05SS has a straight section of the storage ring, where IDs for light sources can be installed. Mechanical design of the vacuum chamber for the ID straight section and conceptual design of IDs have been started.

The study of the production of  $\gamma$ -ray photons with energies of the order of 10 MeV is in progress in BL38B2 and BL05SS. The  $\gamma$ -ray photons are generated *via* backward Compton scattering of optically pumped far-infrared laser photons by electrons of the storage ring.

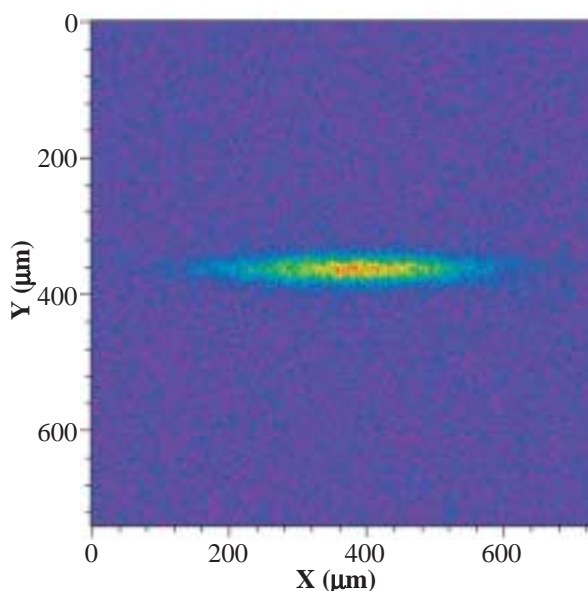


Fig. 4. Example of images of the electron beam of the storage ring observed using the zone plate X-ray beam profile monitor.

## Installation of 10T Superconducting Wiggler for Beam Tests

There are some demands for  $\gamma$ -rays in the energy range from a few hundred keV to several or ten MeV. Use of high-energy photons of about a few hundred keV to 500 keV will become possible in Compton scattering experiments. Intense low-energy positron beams can be produced via the electron-positron pair-production process by  $\gamma$ -rays. To generate such  $\gamma$ -rays, a 10 T superconducting wiggler (SCW) was proposed [6], a prototype machine fabricated in Budker INP [7] and was tentatively installed in the storage ring in August 2002, and beam tests were carried out [8]. Figure 5 shows a photograph of the SCW installed in the storage ring. Basic parameters of the SCW are listed in Table I.

Number of Poles:	3
S/C Wire:	Nb <sub>3</sub> Sn and NbTi
Maximum Field:	10 T
Stored Energy at 10T:	400 kJ
Weight:	1000 kg
Length:	1 m
Pole Gap:	42 mm
Beam Chamber:	65 mm(H) × 20 mm(V)

After ramping up the magnetic field of SCW to 9.7 T, we could successfully store a beam in the storage ring. The stored current was limited to 1 mA to avoid high heat load on photon absorbers and radiation damage to accelerator components. We then measured beam parameters such as horizontal beam size (Fig. 6), bunch length and tune shift affected by the strong magnetic fields. The results agreed well with calculations based on the measured magnetic field distribution of the SCW. We also measured a spectrum of high-energy SR using the NaI(Tl) scintillator and a photomultiplier at the SCW peak field of 9.5 T. The data was taken at an extremely low beam current of about 8 pA and we could see a reasonable agreement between the experimental data and simulations.

After the beam tests, the SCW was removed from the storage ring and is now in the test bench. When we consider its effects on the stored beam together with the high heat load, it is not easy to use the SCW during user operation. Nevertheless, the applications of high-energy  $\gamma$ -rays generated by the SCW are interesting and important, and we are now looking for a possible way of using the SCW for actual applications.



Fig. 5. Photograph of the SCW.

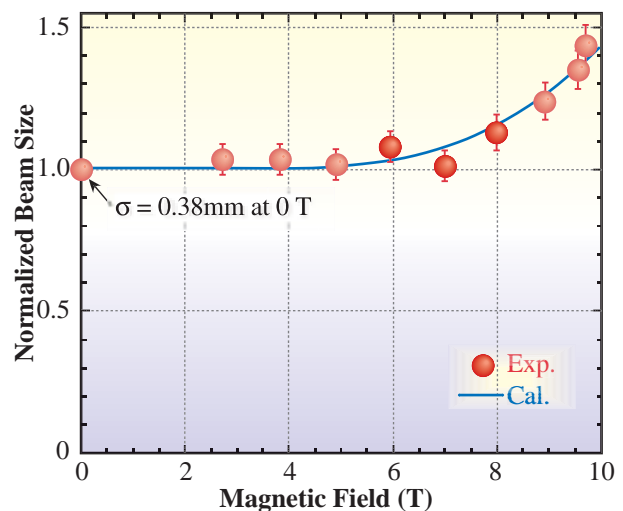


Fig. 6. Horizontal beam size normalized by a value at 0 T.

### HOM-damped Re-entrant Quasi-half-cell RF Cavity for the SPring-8 Storage Ring [9]

The RF cavity parasitic narrow-band coupling impedances of higher order resonant modes (HOMs) cause coupled-bunch instabilities (CBIs) harmful for storing an electron beam. In order to cope with CBIs, the bell-shaped single-cell RF (BSR) of SPring-8 cavities was designed to have lower HOM coupling impedances than the threshold coupling impedance of CBI at a beam current of 100 mA and delivered with systematic modification in their inner size, two frequency tuners and precisely temperature-controlled cooling water [10]. However, a large increase in beam current reduces the threshold coupling impedance of CBI and becomes difficult for the BSR cavities. Therefore, in preparation for the future reinforcement of beam current, a new RF cavity with lower HOM coupling impedances than those in the BSR cavity was designed and its RF properties were examined by the MAFIA frequency-domain simulation. The newly designed RF cavity has a

higher beam accelerating shunt impedance of the TM010 mode than that in the BSR cavity and 3 structures for suppressing CBIs: a re-entrant quasi-half-cell body, HOM skew-imposing ports (SKIPs) and a grooved-beam pipe (GBP). To confirm the designed RF performance of the re-entrant quasi-half-cell RF (RQR) cavity, an aluminum model cavity shown in Fig. 7 was fabricated and the low-power RF measurement was carried out. The measured resonant frequency, Q-value, and R/Q of the TM010 mode in the aluminum model cavity were about 506.9 MHz, 19000 and 200 Ω, respectively. Table II shows the measured RF properties in the model cavity with SKIPs and GBP. These measured values were approximately similar to those obtained by the MAFIA calculations, and the HOM damping performance of the RQR cavity with SKIPs and GBP was verified by the measurement.

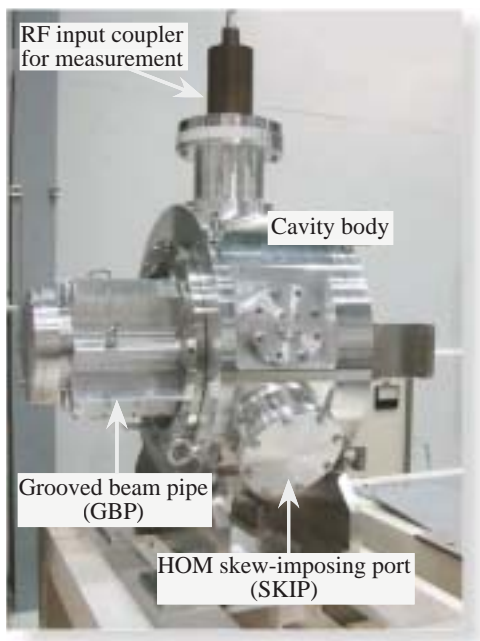


Fig. 7. RQR model cavity made of aluminum.

**Table II. Measured RF properties of the principal resonant modes in the aluminum model RQR cavity with SKIPs and GBP**

mode	frequency [MHz]	Q	coupling coefficients
TM010	506.903 (506.855)	19200 (19800)	2.9
TM110-L	810.888 (816.810)	400 (500)	0.1
TM110-H	819.598 (825.757)	400 (400)	0.1
TM011	919.330 (913.144)	12700 (15600)	7.5
TM111-L	1142.981 (1145.318)	600 (900)	0.2
TM111-H	1145.211 (1149.825)	600 (800)	0.3